Journal of
Nanoscience and Nanotechnology
Vol. 7, 1–5, 2007

Sn-Catalyzed Growth of MgO Nanowires

Hyoun Woo Kim*, Seung Hyun Shim, and Jong Woo Lee

School of Materials Science and Engineering, Inha University, Incheon 402-751, South Korea

We reported the fabrication and characterization of MgO nanowires, which were grown by thermal evaporation of the mixture of MgB_2 and Sn powders at 800 °C through a vapor-liquid-solid (VLS) process. We characterized as-synthesized MgO nanowires using X-ray diffraction, scanning electron microscopy, and transmission electron microscopy. Sn nanoparticles were located at the tips of the nanowires, serving as catalyst for the growth of MgO nanowires. The produced nanowires were of cubic MgO structures with diameters in the range of 10–170 nm. The PL measurement with a Gaussian fitting exhibited visible light emission bands centered at 403, 576, and 720 nm.

Keywords: Nanowires, MgO, Sn-Catalyst.

1. INTRODUCTION

In recent years, one-dimensional (1D) nanostructures (nanotubes, nanobelts, nanowires, and nanorods) have been the focus of extensive research due to their distinctive geometries, novel physical and chemical properties, and promising applications in numerous areas including nanoscale electronics and photonics.[1,2] Accordingly, highly anisotropic 1D nanostructures using various materials, such as carbon, metals, oxides, sulfides, nitrides, etc., have been fabricated through a variety of methods. Furthermore, with the development of the nanotechnology, the demand not only to synthesize a wide variety of 1D nanomaterials but also to develop the novel fabrication method has been increased.

Magnesium oxide (MgO) is a typical wide-band-gap insulator, having found many applications as catalysis, additives in refractory, paint and superconductor products, and substrates for thin film growth.[3,4] In particular, MgO whisker has recently been developed as an intensifier used in superconductive and spaceflight composite materials. Accordingly, many research groups have reported on the synthesis of 1D MgO nanostructures by various techniques including sol-gel process[5] and thermal heating method using MgO powders,[6] a solid mixture of MgO/graphite,[7] MgB_2 powders,[8,9] and Mg metals or powers.[10–13] Recently, MgO nanostructures have been obtained using the Al_2O_3 matrix containing MgO and Co via the Co-catalyzed vapor-liquid-solid (VLS) process.[14] In this paper, a novel method to prepare MgO nanowires is reported, in which we fabricated MgO nanowires based on Sn-catalyzed process, using the mixture of Sn metal powder and MgB_2 nanopowders as the source material. Compared to previously used high-melting-point metal catalyst (such as Au, Ag, and Co), Sn is a relatively cheap metal which is easily removable due to its low melting point. Accordingly, we suggest that the use of Sn not only extends the conventional VLS mechanism to a broad range but also provides a new way for nanowire growth for commercial production.

2. EXPERIMENTAL DETAILS

The synthesis of nanostructures was carried out in a high-temperature tube furnace, which has been described elsewhere.[15] A quartz tube was placed horizontally inside the tube furnace. Sn metal powders and MgB_2 nanopowders with weight ratio of 1:1 (approximately 2 g in total) were fully mixed and then used as the source material. The mixture powders were placed at the lower holder in the center of the quartz tube. The Si plate was placed at the upper holder, which acted as a substrate for collecting the growth products. The vertical distance between the powders and the substrate was approximately 10 mm. The substrate temperature was set to 800 °C. In ambient gas with a constant total pressure of 2 Torr, the typical percentage of O_2 and Ar partial pressure, respectively, were set to approximately 3 and 97%. After 1 h of typical deposition process, the substrate was cooled down and then removed from the furnace for analysis.

The samples were observed and analyzed using glancing angle (0.5°) X-ray diffraction (XRD, X'pert MPD-Philips with Cu$K\alpha_1$ radiation), scanning electron

*Author to whom correspondence should be addressed.

RESEARCH ARTICLE

microscopy (SEM, Hitachi S-4200), and transmission electron microscopy (TEM, Philips CM-200) with energy-dispersive X-ray (EDX) spectroscopy attached. TEM samples were prepared by sonicating the substrate in acetone by ultrasonic treatment. A drop of the dispersion solution was then placed on a porous carbon film supported on a copper (Cu) microgrid. Photoluminescence measurement (PL) was conducted at room temperature in a SPEC-1403 photoluminescence spectrometer with the 325 nm line from a He-Cd laser (Kimon, 1K, Japan).

3. RESULTS AND DISCUSSION

We have examined the morphology and size of resulting product by observing SEM images. Figure 1(a) shows the typical SEM image, indicating that the product consists of a large quantity of 1D structures. Furthermore, statistical analysis of many SEM images revealed that as-synthesized 1D structures had average diameters in the range of 10–170 nm. It is noteworthy that the 1D structures have a particle at the tip, with its diameter ranging from 30 to 500 nm. Figure 1(b) shows an enlarged SEM image, revealing that the tip particles are nearly ball-shaped. The diameter of the solidified spherical droplet at the tip is apparently bigger than the width of the nanowire.

TEM was employed for further structural study of the sample. Figure 2(a) shows a low-magnification TEM image, revealing that the product consists of an agglomeration of nanowires with dark particles attached, agreeing with the SEM observation. The diameters of nanowires and particles in Figure 2(a) are modulated in the range of 10–80 nm and 30–480 nm, respectively. Figure 2(b) exhibits the TEM image of a single nanowire. The clear contrast variation between tip and stem suggests that the tip and the main body of nanowires may consist of different materials. Figure 2(c) is a lattice-resolved high-resolution TEM (HRTEM) image enlarging an area indicated by Arrow 1 in Figure 2(b). The lattice fringe distance is approximately 0.279 nm, which is in coincidence with $(0\bar{1}1)$ plane of tetragonal Sn. The tip particle is covered by a very thin amorphous layer with a thickness of approximately 4 nm. The diffraction spots can be indexed

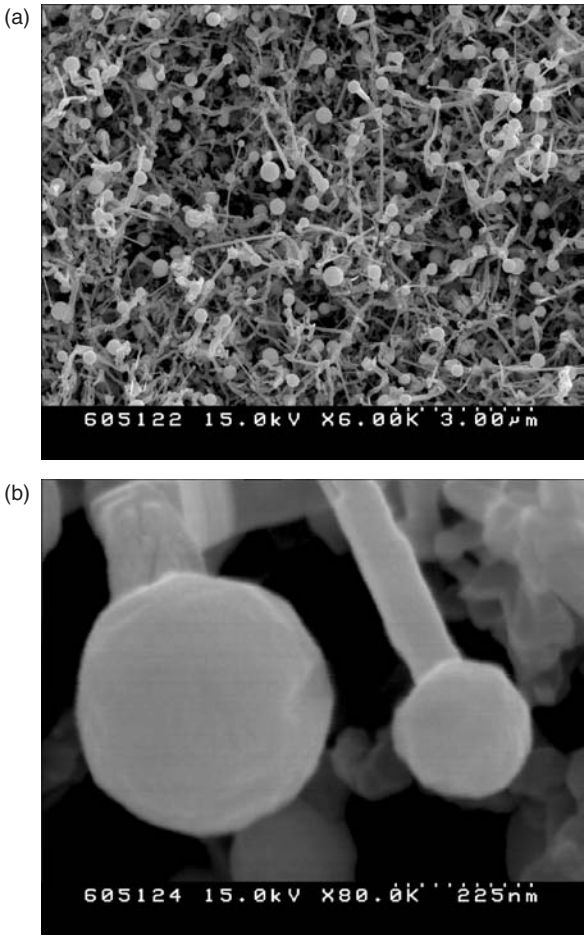

Fig. 1. (a) SEM image of as-synthesized product. (b) Enlarged SEM image of nanowires with tip particles.

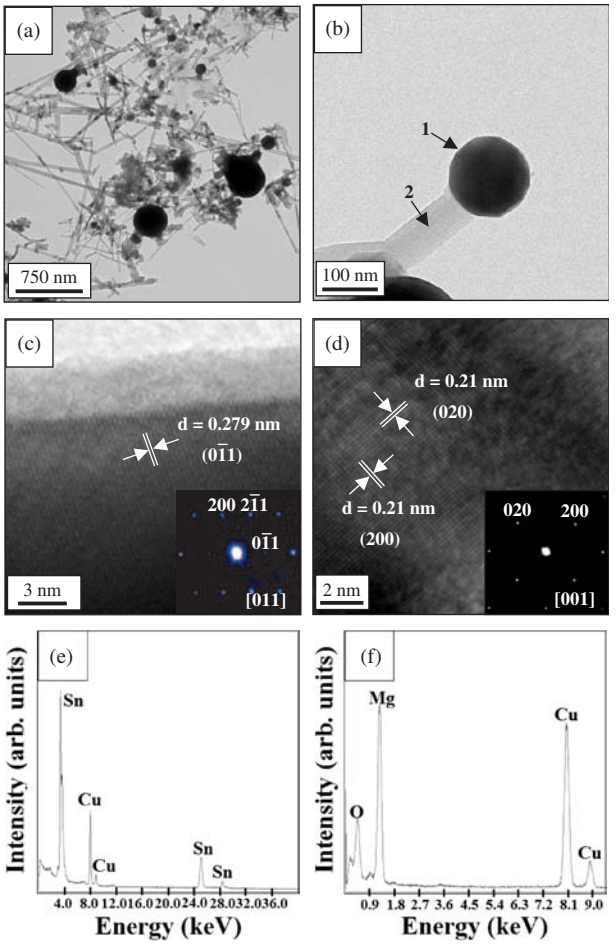

Fig. 2. (a) Low-magnification TEM image of the as-synthesized product. (b) TEM image of a single nanowire. (c, d) HRTEM images corresponding to areas indicated by (c) Arrow 1 and (d) Arrow 2 in (b) (Insets: associated SAED patterns). EDX spectra of (e) the wire tip and (f) the wire stem.

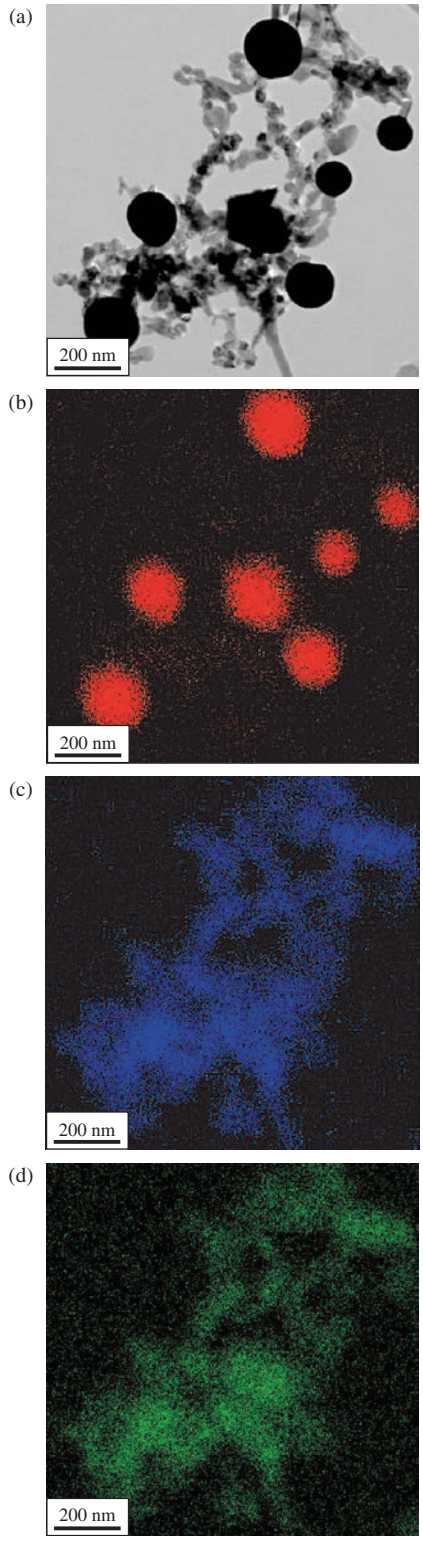

Fig. 3. (a) Low-magnification TEM image of nanowires. Elemental maps of (b) Sn, (c) Mg, and (d) O concentrations.

as (200), (2$\bar{1}$1), and (0$\bar{1}$1) reflections for the [011] zone axis according to the tetragonal structure of Sn.

Figure 2(d) is an HRTEM image corresponding to an area indicated by Arrow 2 in Figure 2(b). The interplanar spacing is approximately 0.21 nm, which correspond to the distance of the neighbouring {200} planes in cubic MgO structure. The lower right inset in Figure 2(d) shows an associated SAED pattern with a [001] zone axis, which indicates the single-crystalline nature of MgO nanowire stems. EDX measurements made on the wire tip and the wire stem indicate that the nanowire tip comprises Sn element, whereas the nanowire stem is composed of Mg and O elements (Figs. 2(e) and (f)). Cu signals are generated from Cu microgrid mesh supporting the nanowires. Figure 3(a) shows a low magnification TEM image of aggregated 1D structures, appearing to have tip-particles. Figures 3(b), (c), and (d) correspond to TEM elemental mapping of Sn, Mg, and O concentrations, respectively, in the structure shown in Figure 3(a). The bright points indicate high concentration of elements. The Mg and O elemental mappings (Figs. 3(c) and (d)) display that both Mg and O are distributed at the stem parts of the nanowires with their absence in the tip region. The Sn elemental mapping (Fig. 3(b)) shows that Sn is concentrated at tip parts of the nanowires. HRTEM images, SAED patterns, EDX spectra, and elemental maps suggest that as-synthesized 1D structures correspond to a Sn-tipped MgO nanowire structure.

An XRD was used to determine the sample phase. Figure 4 displays the typical XRD spectrum of the product. The diffraction peaks of (200), (220), and (222) in this spectrum correspond to the cubic MgO structure with a lattice constant of $a = 0.421$ nm (JCPDS: 04-0829), whereas (200), (101), (220), (211), (301), (400), (321), (420), (411), and (312) peaks can be indexed as tetragonal Sn structure with lattice constants $a = 0.583$ nm and $c = 0.318$ nm (JCPDS: 04-0673). In addition, some weak lines are found to coincide with (110) peak of the tetragonal structure of SnO_2 (JCPDS File No. 21-1250) and with (311) and (400) peaks of the cubic structure of Mg_2SnO_4 (JCPDS File No. 24-0723). XRD analysis confirms the existence

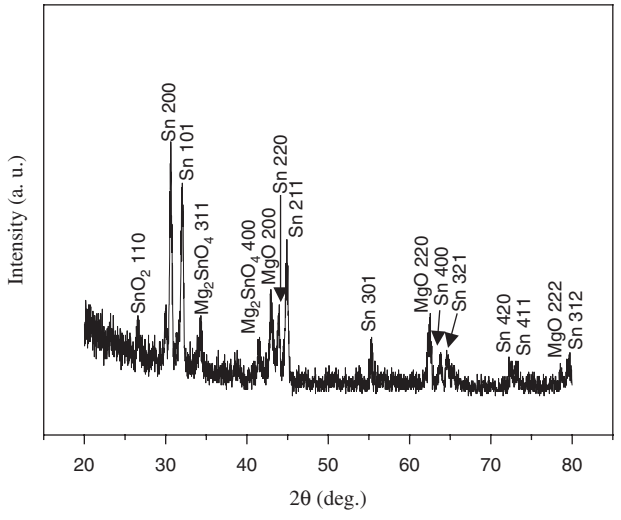

Fig. 4. XRD pattern of the product.

RESEARCH ARTICLE

of MgO and Sn structures, presumably from nanowire stems and tips, respectively. In addition, there exist some compound structures of SnO_2 and Mg_2SnO_4 in the products.

With the solidified spherical droplets at the tips of the nanowires being commonly considered to be the evidence for the operation of the VLS mechanism, the above experimental results suggest that Sn can serve as an effective catalyst for the growth of crystalline MgO nanowires via a VLS process.[16] In the present experiments, the Sn particles are liquid droplets at the growth temperature due to their low melting point (232 °C), serving as energetically favored sites. It is generally agreed that SnO forms at the initial stage of oxidation of liquid Sn around 600 °C.[17] Subsequently, the metastable SnO may decompose to solid SnO_2 and liquid Sn. Previous studies indicate that MgB_2 can decompose at around 800 °C,[8] generating Mg vapor. Also, the most likely source of oxygen may come from the O_2 in the carrier gas, while the oxygen adsorbed on the Si wafer due to air exposure during the processing and the residual oxygen in the tube can be other sources. Herein, we suggest that the growth process can be broken down to several steps. In the first step, solid SnO_2 are deposited on the substrates, possibly in the form of film-like or cluster-like structures. When the synthesis was carried out under the similar conditions in the absence of MgB_2 powders, we obtained the SnO_2 structures. Subsequently, MgB_2 starts to decompose. Since Figures 2 and 3 reveal that most nanowire stems consist of MgO, we suggest that gaseous SnO tends to be transformed into MgO rather than SnO_2, according to the following reaction: $SnO(g) + Mg(g) \rightarrow MgO(g) + Sn(l)$ and thus the generation of solid SnO_2 can be suppressed. The other possibility is that considerable amounts of Sn powders have been consumed during the first step. In the second step, not only MgO vapor but also Mg atoms, O atoms, SnO vapor from the surroundings will adsorb on the Sn droplet to form a Sn–Mg–O liquid alloy and subsequently, the short MgO nuclei precipitate from the solid/liquid interface when the concentration of Mg and O atoms in the alloy droplet is greater than the saturation threshold. In the third step, by continuously dissolving the incoming vapor species, short MgO nuclei will subsequently grow into MgO nanowires. However, the formation mechanism of Mg_2SnO_4 phase is not clear (Fig. 4). One possibility is that MgO reacts with predeposited SnO_2 to form the Mg_2SnO_4 phase. The other possibility is that a trace amount of Mg_2SnO_4 phase has been precipitated from the Sn–Mg–O liquid alloy droplet. Similar to the present work, previous works report that ZnO nanowires[18] and silica nanowires[19] have also been synthesized by using Sn as a catalyst. Further investigation is underway to better understand the detailed growth mechanism.

The room-temperature PL spectrum is presented in Figure 5. In order to have closer insights for the origin of emission regarding the broad band which can be

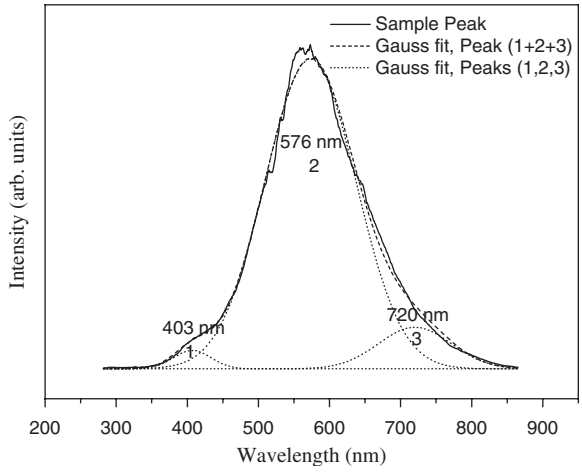

Fig. 5. PL spectrum of as-synthesized product. The light source was the 325 nm-wavelength line from a He-Cd laser.

a superimposition of several peaks, we have fitted the spectral feature with Gaussian functions. The best fit of the emission was obtained with three Gaussian functions, which are centered at 403, 576, and 720 nm, respectively. First, the violet emission (at 403 nm) may be attributed to SnO_2, with the peak being analogous to the emission from the SnO_2 nanocrystalline films.[20] Secondly, the product has a strong peak centered at around 576 nm in the yellow-green region (corresponding to 2.16 eV). The yellow-green light emission spectrum is similar to that of SnO_2 nanomaterials previously synthesized using laser ablation[21] and solution phase growth.[22] Visible light emissions of SnO_2 are known to be related to defects or nanocrystal grains or to defect levels associated with oxygen vacancies or tin interstitials.[20–22] Thirdly, we observe the red peak at about 720 nm, with similar red emission having been observed in the PL spectrum from MgO nanobelts fabricated by the thermal evaporation of Mg powders.[23] The red light emission is known to be related to the relaxation luminescence of defect centers in MgO.

4. CONCLUSION

We have synthesized the MgO nanowires by heating the MgB_2 powders via Sn powder as catalyst. The process appears to be attributed to a VLS mechanism, due to the presence of solidified spherical Sn particles at the tips of the nanowires. HRTEM, SAED, EDX, and elemental mapping analyses show that nanowire stem and tip correspond to cubic MgO and tetragonal Sn structures, respectively. The PL measurement with the Gaussian fitting shows apparent visible light emission bands centered at 403, 576, and 720 nm. The violet and yellow-green emission may be attributed to the SnO_2 structures in the product, whereas the red emission evidently originates from the MgO nanowires. The method reported here may be exploited to produce nanowires of other materials by using Sn as catalyst.

Acknowledgments: This work was supported by Inha Research Fund 2006.

References and Notes

1. X. F. Duan, Y. Huang, Y. Cui, J. Wang, and C. M. Lieber, *Nature* 409, 66 **(2001)**.
2. M. H. Huang, S. Mao, H. Feick, H. Q. Yan, Y. Y. Wu, H. Kind, E. Weber, R. Russo, and P. D. Yang, *Science* 292, 1897 **(2001)**.
3. S. H. C. Liang and I. D. Gay, *J. Catal.* 101, 293 **(1986)**.
4. P. D. Yang and C. M. Lieber, *Science* 273, 1836 **(1996)**.
5. G. Kordas, *J. Mater. Chem.* 10, 1157 **(2000)**.
6. C. O. Hulse and W. K. Tice, *Nature* 206, 79 **(1965)**.
7. P. Yang and C. M. Lieber, *J. Mater. Res.* 12, 2981 **(1997)**.
8. Y. Yin, G. Zhang, and Y. Xia, *Adv. Funct. Mater.* 12, 293 **(2002)**.
9. K. L. Klug and V. P. Dravid, *Appl. Phys. Lett.* 81, 1687 **(2002)**.
10. Y. Li, Y. Bando, and T. Sato, *Chem. Phys. Lett.* 359, 141 **(2002)**.
11. M. Zhao, X. L. Chen, X. N. Zhang, H. Li, H. Q. Li, and L. Wu, *Chem. Phys. Lett.* 388, 7 **(2004)**.
12. S. Car and S. Chaudhuri, *J. Nanosci. Nanotechnol.* 6, 1447 **(2006)**.
13. L. Hu, Y. X. Li, J. P. Qu, Z. X. Huang, X. T. Huang, X. X. Ding, C. Tang, and S. R. Qi, *J. Nanosci. Nanotechnol.* 4, 1071 **(2004)**.
14. Y. Q. Zhu, W. K. Hsu, W. Z. Zhou, M. Terrones, H. W. Kroto, and D. R. M. Walton, *Chem. Phys. Lett.* 347, 337 **(2001)**.
15. H. W. Kim, N. H. Kim, J. H. Myung, and S. H. Shim, *Phys. Stat. Sol. (a)* 202, 1758 **(2005)**.
16. R. S. Wagner and W. C. Ellis, *Appl. Phys. Lett.* 4, 89 **(1964)**.
17. D. W. Yuan, R. F. Yan, and G. Simkovich, *J. Mater. Sci.* 34, 2911 **(1999)**.
18. P. Gao and Z. L. Wang, *J. Phys. Chem. B* 106, 12653 **(2002)**.
19. S. Sun, G. Meng, M. Zhang, Y. Hao, X. Zhang, and L. Zhang, *J. Phys. Chem. B* 107, 13029 **(2003)**.
20. T. W. Kim, D. U. Lee, and Y. S. Yoon, *J. Appl. Phys.* 88, 3759 **(2000)**.
21. J. Hu, Y. Bando, Q. Liu, and D. Golberg, *Adv. Func. Mater.* 13, 493 **(2003)**.
22. B. Cheng, J. M. Russell, W. Shi, L. Zhang, and E. T. Samulski, *J. Am. Chem. Soc.* 126, 5972 **(2004)**.
23. J. Zhang and L. Zhang, *Chem. Phys. Lett.* 363, 293 **(2002)**.

Received and Revised/Accepted: 5 April 2007.